



PERGAMON

Corrosion Science 44 (2002) 2231–2242

**CORROSION**  
**SCIENCE**  
www.elsevier.com/locate/corsci

## Characterization of protective rust on ancient Indian iron using microprobe analyses

P. Dillmann <sup>a</sup>, R. Balasubramaniam <sup>b,\*</sup>, G. Beranger <sup>c</sup>

<sup>a</sup> *Laboratoire Pierre Sûe CEA/CNRS, CE Saclay 91191-Gif sur Yvette Cedex, France*

<sup>b</sup> *Department of Materials and Metallurgical Engineering, Indian Institute of Technology, Kanpur 208016, India*

<sup>c</sup> *Université de Technologie de Compiègne, Laboratoire Roberval, BP 529, 60205 Compiègne Cedex, France*

Received 4 June 2001; accepted 8 January 2002

---

### Abstract

Local compositional and structural information was obtained from an ancient 1500-year-old Indian iron and its protective scale utilizing microprobe techniques ( $\mu$ XRD and  $\mu$ PIXE). Different locations in the iron matrix and in the entrapped slag inclusions were also analyzed for P contents. The P content of the metallic iron matrix was very heterogeneous. Lower P contents were observed in the regions near slag inclusions. The surface oxide scales was layered. Enrichment of P in the metal–scale interface and in the scale adjacent to the interface was determined. The P content in the scale decreased on moving away from the interface. Microdiffraction patterns obtained at different locations in the oxide scale indicated that at locations where the P content was high (i.e. nearer the interface), the oxide was amorphous while at locations where P was low, crystalline phases were identified. The presence of crystalline phosphates was also confirmed at some regions in the scale, where the P content was relatively very high. The probable reasons for the presence of the identified phases in the atmospheric corrosion product have been discussed. © 2002 Elsevier Science Ltd. All rights reserved.

*Keywords:* Ancient Indian iron; Atmospheric corrosion; Rust characterization; Microdiffraction;  $\mu$ PIXE; Phosphorous concentration profiling

---

---

\* Corresponding author.

## 1. Introduction

The causes for the excellent atmospheric corrosion resistance of ancient Indian iron have been debated for several decades. A good example of this excellent resistance is the Delhi iron pillar (DIP), a 1600-year-old structure that has withstood significant corrosion damage. A detailed characterization of the oldest DIP rust [1] has established that the DIP obtains its excellent corrosion resistance due to the formation of a protective crystalline iron hydrogen phosphate hydrate at the interface between the metal and the atmospheric rust [2]. One of the reasons for the formation of this phosphate is the availability of a significant amount of P in the underlying metal. Based on several reported analyses, the average P content in the DIP has been reported to be 0.24% [2]. Available compositions from ancient Indian iron objects indicate relatively high P contents [3,4]. One probable reason for the observed high P contents could be the use of P containing ore and/or charcoal. Thermodynamic and thermal analyses show that the type of slag in the ancient iron-making shaft furnaces influenced the P content of the metal [5]. The ideal requirements for dephosphorization are well established: high oxygen potential and high slag basicity (creating a low activity coefficient for phosphorus in the slag) [6]. Moreover, the efficient dephosphorization capacity of CaO is well-recognized [7]. Ancient Indian iron-making furnaces did not utilize limestone in the charge and therefore, CaO was not available in the slag. In the absence of CaO in the slag, a greater amount of P would be retained in the metal.

The corrosion products that can be observed on mild steels exposed to atmospheres (without chloride ions) are well known for relatively short exposure times:  $\alpha$ -FeOOH (goethite),  $\gamma$ -FeOOH (lepidocrocite),  $\text{Fe}_{3-x}\text{O}_4$  (magnetite) and X-ray amorphous matter [8–10]. In the case of P-containing weathering steels, Misawa and co-workers [8,9] have proved the formation of amorphous  $\delta$ -FeOOH utilizing Fourier transform infrared spectroscopy (FTIR). Other workers [11,12] have also independently confirmed this. In P-containing weathering steels, the initial corrosion of the matrix leads to the enrichment of P at the metal–scale interface. In the presence of P at this interface, the formation of a compact layer of amorphous  $\delta$ -FeOOH layer is favored in this region. Moreover, experiments have shown that  $\text{H}_2\text{PO}_4^-$  ions prevent crystal growth of the corrosion products [8,9]. With prolonged exposure, enrichment of P in the  $\delta$ -FeOOH layer continues and this has been also observed in P-containing weathering steels [8,9]. Over relatively longer periods of time, this enrichment leads to the precipitation of insoluble phosphates, as has been found in the DIP rust [1,2]. Alternate wetting and drying conditions have further effect on the nature of the surface films. For example, alternate wetting and drying cycles lead to crystallization of the phosphate in the case of the DIP rust [2] and this crystalline phosphate is more protective due to the large decrease in its porosity on crystallization. Therefore, the superior corrosion resistance of P- and Cu-containing weathering steels has been attributed to this compact  $\delta$ -FeOOH layer next to the metal surface, which is also enriched with the element(s) added to provide weathering resistance. While the  $\alpha$ -FeOOH and  $\gamma$ -FeOOH can be identified by X-ray

diffraction, it is generally not possible to identify the  $\delta$ -FeOOH phase by this characterization technique [8,9]. In normal mild steels, the  $\delta$ -FeOOH phase forms in a discontinuous manner and does not offer protection against atmospheric corrosion.

It is important to multiply investigations on corrosion-resistant ancient iron artifacts (containing P) in order to elucidate the role of phosphorus in long-term atmospheric corrosion mechanisms. The composition and structure of ancient irons are generally heterogeneous in nature because of the nature of ancient iron-making processes [2]. Ancient iron can contain numerous second phase particles (slag inclusions). Moreover, the composition of minor elements (like C, P, Mn, etc.) can vary significantly from one location to another. Therefore, it is important to compositionally analyze the material at different locations in order to examine the variation of the minor element compositions. Microprobe analyses are necessary to perform these investigations. Moreover, the nature and structure of the surface rust are influenced by the composition of the metallic matrix. Therefore, it is also important to investigate the structural variations in surface scales. The present paper outlines the application of several microprobe (compositional and structural) analysis techniques to investigate the metal and the surface atmospheric corrosion product in an iron clamp obtained from an ancient Gupta temple (now in ruins) at a site called Eran in Madhya Pradesh in central India. Inscriptions in the site indicate that the temple was constructed in the later half of the fifth century AD [14]. The aqueous corrosion behavior of this iron has been studied [15] and its atmospheric corrosion products characterized [16] earlier by FTIR and Mössbauer spectroscopy. Scanning electron microscopy revealed a two-layered surface scale and EPMA analysis near the metal–scale interface indicated a higher P content at this location when compared to that in the matrix [16]. The aim of the present paper is to characterize the structural (using microdiffraction techniques utilizing focused synchrotron radiation) and compositional (using microprobe techniques) variation in the oxide scale.

## 2. Experimental procedure

Two different sample preparation methods were utilised, depending on the analysis technique. In the first method, a transverse section of the sample was prepared after mounting the specimen in epoxy resin, and polished with SiC paper (grades 180 through 2500) and diamond paste (3 and 1  $\mu\text{m}$ ). This mounted specimen was observed in a Cambridge Stereoscan 120 scanning electron microscope (SEM) and by an optical microscope (OM). The same sample was also utilized for analysis with the nuclear microprobe of the Pierre Süe Laboratory (CE Saclay, France) for proton induced X-ray emission (PIXE) spectrometry analyses. The X-ray microdiffraction ( $\mu\text{XRD}$ ) analysis, performed at Laboratoire pour l'Utilisation du Rayonnement Electromagnétique (LURE), Orsay, France, required to be conducted in the transmission mode. Therefore, a thin film, of 20  $\mu\text{m}$  thickness, was prepared with another

transverse section of the sample mounted in epoxy resin. In order to accomplish this, first, a slide of the mounted sample was cut with a diamond cutting wheel. This slide was later mechanically trimmed and polished with 1200 grade SiC paper. The final thickness of the thin film obtained was about 50  $\mu\text{m}$ . One of the faces was fine polished with 3  $\mu\text{m}$  diamond paste so that it could be observed with an Olympus OM. The thin film was deposited on a 30  $\mu\text{m}$  kapton scotch tape. The final sample was carbon coated by sputtering. In this way, the thin film was first observed in the OM and SEM, and later specific local regions of interest were investigated by  $\mu\text{XRD}$ . In addition to the metallographic structure observation, the major elements in the slag inclusions and in the oxide scales were detected by energy dispersive spectrometry (EDS), coupled to the SEM operating at 20 keV, using a Si(Li) detector with a thin beryllium window.

To detect minor and trace elements in the material, the  $\mu\text{PIXE}$  method was utilized. This method is convenient to chemically analyze samples because it permits quantification of relatively low amounts of elements ( $Z$  higher than 12) in the metallic matrix and also allows simultaneous multi-elemental analyses [17]. This aspect is important specially when studying archaeological iron samples because they usually contain heterogeneous concentrations of minor elements. A 1.5 MeV proton beam was used. This energy was selected to favor the X-ray emission corresponding to the lighter elements. The beam current was about 150 pA for a  $2 \times 2 \mu\text{m}^2$  beam spot size. The distance between the sample and the X-ray Si(Li) detector (positioned at  $45^\circ$  from the incident beam) was 6 cm. A 15  $\mu\text{m}$  Mylar filter was used to reduce Fe pill-up peaks. The data collected were analyzed with the GUPIX 99 program. The relative error obtained on the quantitative results is about 5%. The profile data were computerized with the RISMIN program. The detailed experimental procedure is provided elsewhere [18]. A reference sample of low-alloyed steel containing 450 ppm phosphorus was utilized.

The  $\mu\text{XRD}$  experiments were conducted on the D15 beamline at LURE. The white X-ray beam delivered by the DCI ring was focused and monochromatized by a carbon/tungsten Bragg Fresnel multilayer lens (BFML). The BFML is a wide band pass monochromator resulting in broadening of the diffraction peaks. Photons centred around 14 keV ( $\lambda = 0.8857 \text{ \AA}$ ) were selected and focused down to a  $10 \times 10 \mu\text{m}^2$  beam. The diffraction patterns were collected with an image plate, downstream from the sample. 1-D diffraction patterns were obtained by circularly integrating diffraction rings using the FIT2D software developed at the European synchrotron radiation facility (ESRF). The reference sample used was silicon powder. The spectra were compared with the JCPDF database using the Diffrac+ program.

### 3. Results and discussion

Several distinct local zones in the ancient Indian iron sample were analyzed: the iron matrix, the entrapped slag inclusions (particularly, the ones that were surrounded by an oxide), and the external oxide scales.

### 3.1. The iron substrate

The phosphorus content was examined at different points of the matrix using the  $\mu$ PIXE method. The P contents, determined at several different locations, are provided in Table 1. Some details about the P contents determined should be noted. First, a wide variation in the P content indicated the heterogeneous nature of the iron matrix. The global P content of the same material (including the P in metal as well as in the slag) was determined by wet chemical analysis and this was found to be 0.25% [15]. However, the P content in the metal can fluctuate from 570 to 2300 ppm depending on the location. Points 7 and 9 were both collected near the metal–oxide interface but at different locations of the sample. The enhancement of P near the metal surface observed by an EPMA [16] is partially verified, although the EPMA study did not report the regions of lower P content. Secondly, the relatively high amounts of P in the Gupta-period ancient Indian iron have to be noted.

A phosphorus concentration profile was obtained with the  $\mu$ PIXE method in the metallic matrix near slag inclusions. As observed in other ancient phosphoric irons [18], the profile revealed decreasing P content near the slag inclusion (for distances less than 10  $\mu$ m). This effect must result due to the dephosphorizing power of the slag. At locations further away from the inclusions (about 40–50  $\mu$ m), the variation in the phosphorus content were similar to that typically observed in the metallic matrix. The slag inclusions were characterized by  $\mu$ XRD and they were composed of wüstite dendrites in a matrix that was partly glassy and partly fayalitic [19]. The glassy part of the matrix was reasoned to be phosphates based on the identification of a significant amount of P in the slag inclusions by EDS analyses [19]. Interestingly, OM and SEM observations and  $\mu$ XRD experiments conducted on an oxide in between the iron matrix and the inclusions that are located near the surface (up to a distance of 100  $\mu$ m from the metal–oxide interface), indicated it was goethite ( $\alpha$ -FeOOH). This oxide was likely to be a corrosion product, as the material had been handled in the atmosphere for some time. This could be either from the slag (wüstite being later converted to goethite) or metal (oxidation of the metallic matrix in the zone surrounding the inclusion). The latter appears more reasonable because wüstite is entrapped in a (relatively stable) fayalitic matrix.

Table 1  
Phosphorus content in the Fe matrix

Point	P (mass ppm)
1	1371
2	1462
3	1151
4	2179
5	1531
6	570
7	2300
8	1309
9	750

Points 7 and 9 were collected from near metal–oxide interfaces at two different locations.

### 3.2. The oxide scale

The compositional variations of P across the atmospheric oxide scale at different locations on the sample were analyzed by  $\mu$ PIXE. The variation in P content as a function of distance into the oxide is presented in Fig. 1. In this figure, three different profiles obtained at three different locations are provided. The profiles based on data points represented by the open and closed squares were obtained at locations where the P content was relatively low in the metallic matrix just below the scale. The profile based on the data points represented by triangles was obtained at a location where the P content was relatively high. These profiles indicated that significant enrichment of P could be obtained in the oxide scale. Notice also, that in certain regions, the oxide thickness could be as high as 800  $\mu\text{m}$ . It is interesting that in the locations where the P content was relatively low in the metallic matrix (square data points in Fig. 1), there was a higher amount of P especially at the scale–metal interface and this continued into the scale. However, with increasing distance into the scale, the P content decreased. The present study clearly proves the enrichment of P content at the metal–scale interface and in the near vicinity of the oxide scale, in regions both rich and poor in P.

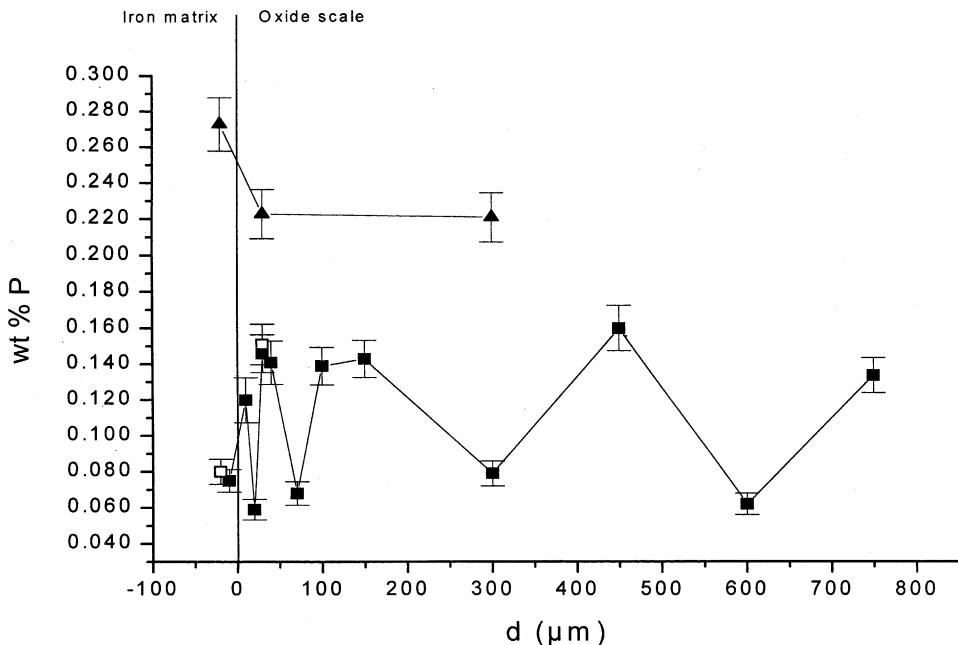


Fig. 1. Variation of P content as a function of distance from the metal–oxide interface. Three different profiles obtained at three different places are provided. The profiles based on data points represented by the open and closed squares were obtained at locations where the P content was relatively low in the metallic matrix just below the scale. The profile based on the data points represented by triangles was obtained at a location where the P content was relatively high.

It was earlier reported that the oxide scale in the same sample was layered [16]. A SEM micrograph was provided where the presence of two layers could be distinguished [16]. The inner layer was optically dull while the outer layer was optically bright [16]. The optical nature of the oxide indicated indirectly the crystalline or amorphous nature of the scale. The layered structure of the protective rust in weathering steels is well established [8,9,13]. Regarding the optical nature of the layers on weathering steels, Okada et al. [20,21] pointed out that the inner optically isotropic layer of the surface rust is composed of X-ray amorphous spinel type iron oxide which can protect the steel matrix. Yamashita et al. [13] also observed, by microscopic observation using reflected polarized light and crossed nicols, that the rust layer present on a weathering steel exposed for 26 years could be divided into two parts: an outer layer which was optically active (i.e. illuminated) and an inner layer which was optically isotropic (darkened). On the other hand, the surface rust formed on mild steels consists of a mottled structure consisting of the optically active and isotropic corrosion products [13]. It is also established that weathering steels obtain their protection due to the presence of the amorphous (dark) inner layer [13]. Therefore, based on the above studies, it was concluded that the inner layer was amorphous while the outer layer was crystalline. The innermost thin layer seen next to the metal surface was proposed to result due to the precipitation of  $\delta$ -FeOOH because of the enrichment of P at this location.

In order to obtain further insights and local information into the nature of the rust in the same sample,  $\mu$ XRD experiments were conducted to understand the phase distribution in the atmospheric rust. Fig. 2 shows a typical oxide scale as observed in

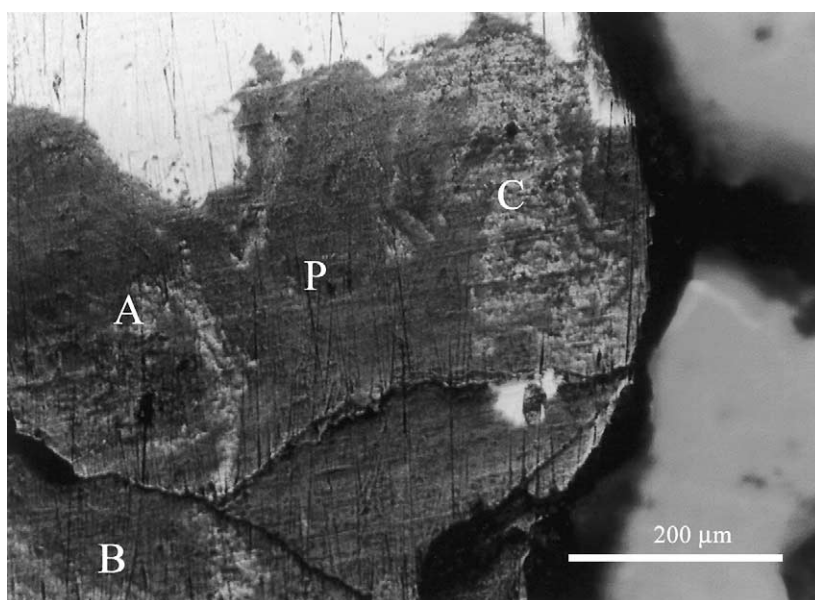


Fig. 2. SEM micrograph showing the transverse section of the oxide scale at a location where the P content was high in the metallic matrix adjacent to the scale–metal interface.

the OM. The local structural variations in the oxide scale were next determined by microdiffraction experiments. As noted before, the P content in the metal adjacent to the surface oxide was also determined. P was not present uniformly in the scale but at certain places, the P concentration attempted 1 wt.%. One such location is marked P in Fig. 2. The  $\mu$ XRD pattern obtained from this location is provided in Fig. 3. The major phases were magnetite (JCPDF 751609) and goethite (JCPDF 81463) but weak diffraction peaks that did not belong to these two phases were also identified. These peaks were in good agreement with the JCPDF pattern (JCPDF 35622) of a crystalline phosphate  $\text{Fe}_2(\text{PO}_4)(\text{OH})$ . In the scale provided in Fig. 2, three different regions were distinguished based on the  $\mu$ XRD experiments. These three regions are marked A, B and C. Interestingly, in region A, in general, no diffraction was obtained indicating that these regions were amorphous in nature. The  $\mu$ XRD pattern obtained from this amorphous region is shown in Fig. 4 from where it can be seen that there are no diffraction peaks on the pattern. On the other hand, microdiffraction from region B (Fig. 5) indicated magnetite (JCPDF 751609) while microdiffraction from region C (Fig. 6) indicated goethite (JCPDF 61463). The matrix near A zone possessed a higher P content. Therefore, these microdiffraction experiments provided significant insights in to the nature of the protective rust on ancient Indian iron. The oxide scales formed near the high P containing metallic matrix consisted of a lower amount of crystalline compounds. On the other hand, when the

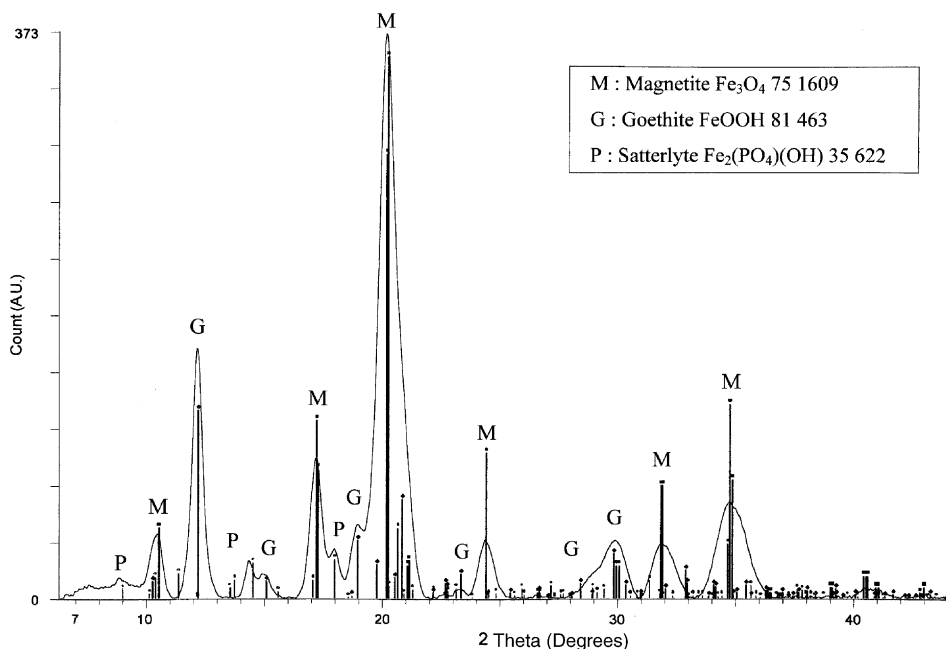


Fig. 3. The  $\mu$ XRD pattern obtained from the location marked P in Fig. 2. The presence of crystalline phosphate was indicated in addition to magnetite and goethite.

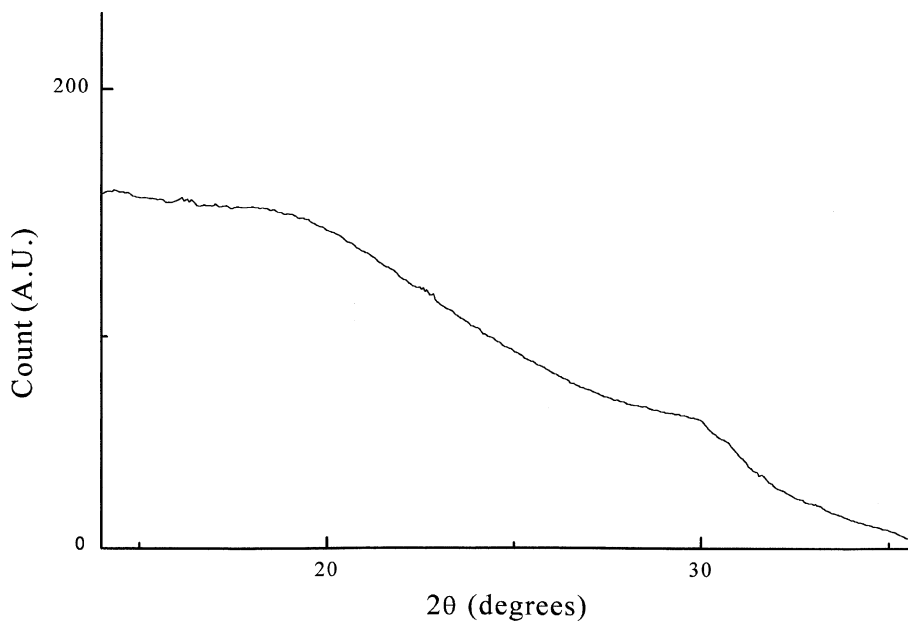


Fig. 4. The  $\mu$ XRD pattern obtained from the location marked A in Fig. 2. There are no diffraction peaks on the pattern indicating the amorphous nature of the oxide at this location.

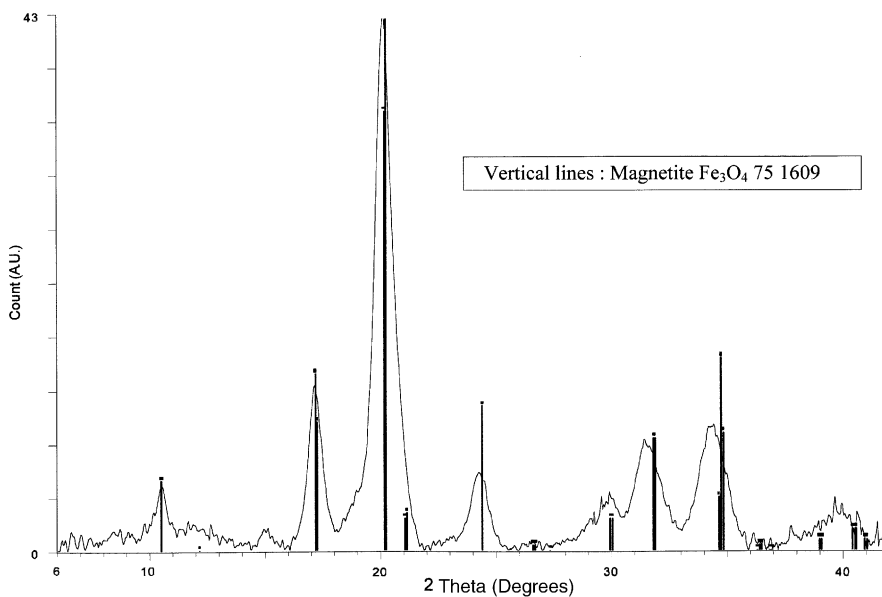


Fig. 5. The  $\mu$ XRD pattern obtained from the location marked B in Fig. 2. The presence of crystalline magnetite was indicated.

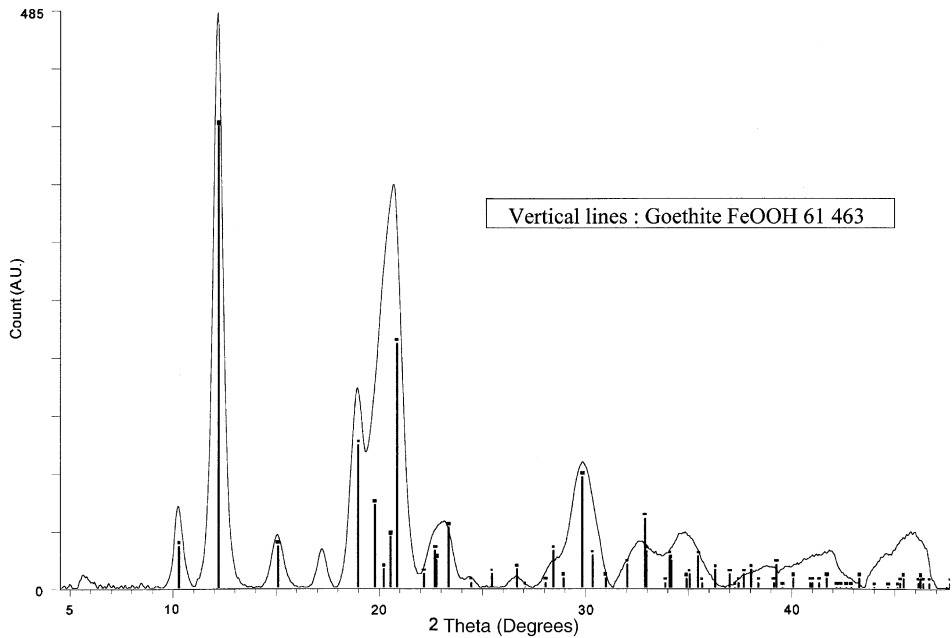


Fig. 6. The  $\mu$ XRD pattern obtained from the location marked C in Fig. 2. The presence of crystalline goethite was indicated.

P-content in the matrix was lower, the usual crystalline atmospheric corrosion products (magnetite and  $\alpha$ -goethite) were determined. Finally, in the locations in the oxide where the P content was relatively high, crystalline phosphates were identified by  $\mu$ XRD. The formation of crystalline phosphate in the surface scales on iron generally occurs either in the presence of oxidizers or due to a large number of wetting-and-drying cycles (i.e. by the process of dissolution and re-precipitation) [22]. The alternate wetting and drying cycles experienced in the atmospheric corrosion process could probably explain the presence of these crystalline phosphates. Fig. 7 provides a schematic summary of the observations.

#### 4. Conclusions

Local compositions and structures were determined from the substrate and surface rust in an ancient 1500 year-old Indian iron using microprobe techniques (EDS,  $\mu$ XRD and  $\mu$ PIXE). Phosphorous contents in the matrix as well as in the oxide scales were not uniform. A relatively low amount of P was detected in the iron matrix adjacent to the slag inclusions. P enrichment at the metal–oxide interface was confirmed. In the locations where the P content was high at the metal–scale interface, the scale was amorphous in nature while in the locations where P content was lower, crystalline iron corrosion products (magnetite and  $\alpha$ -goethite) were identified.

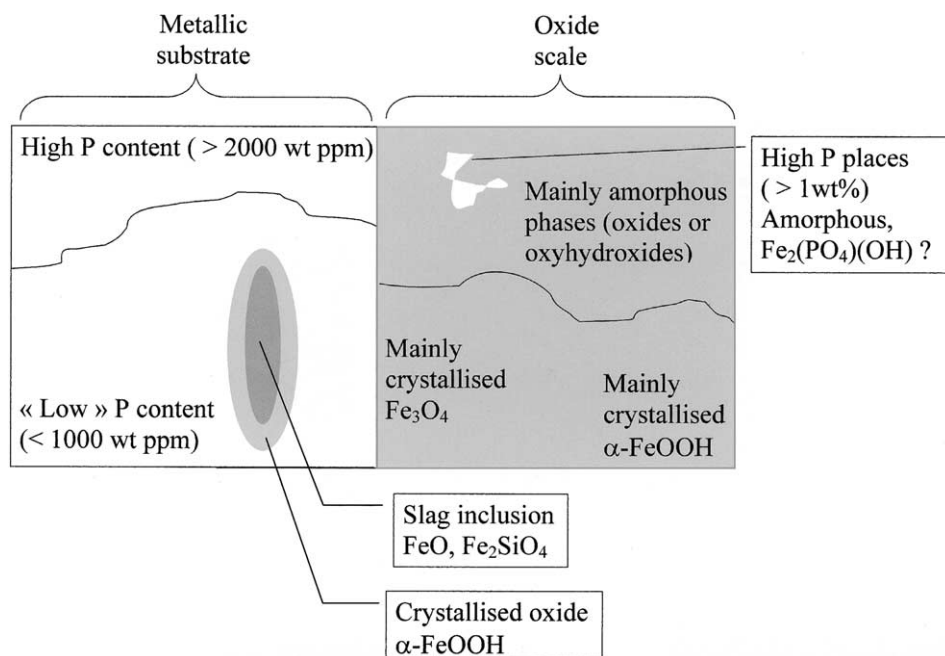


Fig. 7. Schematic summary of the local observations made on the iron clamp.

Crystalline phosphates were identified in locations in the oxide scale where the P content was high. Microprobe techniques are advantageous to understand the local structures of protective films that form on atmospheric exposure.

### Acknowledgements

The authors would like to thank the Archaeological Survey of India for their cooperation.

### References

- [1] R. Balasubramaniam, A.V. Ramesh Kumar, Characterization of Delhi iron pillar rust by X-ray diffraction Fourier infrared spectroscopy and Mössbauer spectroscopy, *Corrosion Science* 42 (2000) 2085–2101.
- [2] R. Balasubramaniam, On the corrosion resistance of the Delhi iron pillar, *Corrosion Science* 42 (2000) 2103–2129.
- [3] B. Prakash, Metallurgy of iron and steel making and blacksmithy in ancient India, *Indian Journal of History and Science* 261 (1991) 351–371.
- [4] B. Prakash, V. Tripathi, Iron technology in ancient India, *Metals and Materials* 2 (1986) 568–579.
- [5] A. Vizcaino, I.J. McColm, J.G. McDonnel, A thermal analysis study of the role of phosphates in the bloomery iron process, *Bulletin of the Metals Museum* 30 (1998-II) 38–55.

- [6] B.J. Monaghan, R.J. Pomfret, K.S. Coley, The kinetics of dephosphorization of carbon saturated iron using an oxidizing slag, *Metallurgical and Materials Transaction B* 29B (1998) 111–118.
- [7] E. Turkdogan, *Fundamentals of Steel Making*, Institute of Materials, London, 1996.
- [8] T. Misawa, T. Kyuno, W. Suetaka, S. Shimodaira, The mechanism of atmospheric rusting and the effect of Cu and P on the rust formation of low alloy steels, *Corrosion Science* 11 (1971) 35–48.
- [9] T. Misawa, K. Asami, K. Hashimoto, S. Shimoaira, The mechanism of atmospheric rusting and the protective rust on low alloy steel, *Corrosion Science* 14 (1971) 279–289.
- [10] I. Suzuki, Y. Kisamatsu, N. Masuko, Nature of atmospheric rust on iron, *Journal of the Electrochemical Society* 127 (1980) 2210–2215.
- [11] H. Kihira, S. Ito, T. Murata, The behaviour of phosphorus during passivation of weathering steel by protective patina formation, *Corrosion Science* 31 (1990) 383–388.
- [12] J.T. Keiser, C.W. Brown, Characterization of the passive film formed on weathering steel, *Corrosion Science* 23 (1983) 251–259.
- [13] M. Yamashita, H. Miyuki, Y. Matsuda, H. Nagano, T. Misawa, The long term growth of the protective rust layer formed on weathering steel by atmospheric corrosion during a quarter of a century, *Corrosion Science* 36 (1994) 283–299.
- [14] R.S. Tripathi, *History of Ancient India*, Motilal Banarsidass Publishers, New Delhi, 1992, pp. 252–253.
- [15] V. Puri, R. Balasubramaniam, A.V. Ramesh Kumar, Corrosion behaviour of ancient 1500-year old Gupta iron, *Bulletin Metals Museum* 28II (1997) 1–10.
- [16] A.V. Ramesh Kumar, R. Balasubramaniam, Corrosion product analysis of ancient corrosion resistant Indian iron, *Corrosion Science* 40 (1998) 1169–1178.
- [17] S.A.E. Johansson, J.L. Campbell, *PIXE a Novel Technique for Elemental Analysis*, John Wiley and Sons, New York, 1988.
- [18] D. Neff, P. Dillmann, Phosphorus localisation and quantification in archaeological iron artefacts by micro PIXE analyses, *Nuclear Instrument and Methods in Physics Research B* 181 (2001) 675–680.
- [19] P. Dillmann, R. Balasubramaniam, Characterization of ancient Indian iron and entrapped slag inclusions using electron photon and nuclear microprobes, *Bulletin of Materials Science* 24 (2001) 317–322.
- [20] H. Okada, Atmospheric corrosion of steels, *Journal of Society of Material Science of Japan* 17 (1968) 705–709.
- [21] H. Okada, Y. Hosoi, K. Yukawa, H. Naito, Structure of the rust formed on low alloy steels in atmospheric corrosion, *Journal of the Iron and Steel Institute of Japan* 55 (1969) 355–365.
- [22] E.L. Ghali, R.J.A. Potoin, The mechanism of phosphating of steel, *Corrosion Science* 12 (1972) 583–594.